ELSEVIER

Contents lists available at ScienceDirect

Fuel Processing Technology

journal homepage: www.elsevier.com/locate/fuproc



Decarboxylative - Dimerization of levulinic acid using spent Li-ion battery electrode material with lithium nickel cobalt manganese oxide as a catalyst

Ananda S. Amarasekara a,b,*, Deping Wang

- ^a Department of Chemistry, Prairie View A&M University, 700 University Drive, Prairie View, TX 77446, USA
- ⁵ Center for Energy and Environmental Sustainability, Prairie View A&M University, 700 University Drive, Prairie View, TX 77446, USA

ARTICLE INFO

Keywords:
Levulinic acid
Dimerization
Metal oxide catalyst
Li-ion battery
Lithium nickel cobalt manganese oxide
Decarboxylation

ABSTRACT

A low cost catalyst prepared by pyrolyzing electrode coating material from spent Li-ion battery cells was shown as an effective catalyst for the decarboxylative - dimerization of levulinic acid to a mixture of C6 and C9 fuel precursors. The highest levulinic acid conversion of 94% was observed with 10% (w/w) catalyst loading under 1.24 MPa H₂ at 140 °C, 15 h. A reaction scheme was proposed to explain the novel transformation producing C9 lactone products and C6 unsaturated alcohol product through a decarboxylative pathway followed by the aldol dimerization of levulinic acid.

1. Introduction

Current efforts to make sustainable carbon based fuels and chemical feedstocks are a high priority research areas with an urgent necessity due to climate change concerns and depleting petroleum reserves. Upgrading of cellulosic biomass derived C5–6 range feedstocks like furfural, 5-hydroxymethylfurfual and levulinic acid (LA) to bio-fuel feedstocks, biofuels or sustainable monomers is a major thrust area in this effort [1,2]. Levulinic acid or 2-oxopentanoic acid is a versatile intermediate in this approach, where it can be produced by depolymerization of cellulose to glucose followed by dehydration - rehydration under acid catalysis [3,4].

Several research teams have explored the dimerization of LA as an approach of upgrading the C5 feedstock to valuable C10 compounds and most studies describe the aim as an approach to produce bio-fuels and particularly bio-jet fuel [5–7]. However all LA dimerized products requires a challenging deoxygenation in conversion to hydrocarbons, and this step has received little attention, [8–11]. The self-condensation reaction of LA can be catalyzed by either bases or acids. Ordonez and co-workers have used a Mg—Zr oxide mixture as a catalyst, where they reported three major products: LA dimer, LA - α -angelica lactone aldol condensation product and α -angelica lactone [12]. However, when NiMo/Al₂O₃ was employed as the catalyst for LA dimerization under H₂ gave 1-oxo-6-methylspiro[4,4]nonan-2-one together with butanone, pentanal, n-butane and n-pentane [13]. The dimerization of LA esters are also known under NaOEt as catalyst to give tetra-substituted

cyclopentadiene [14]. Where Li et al. claimed that these substituted cyclopentadienes can be catalytically reduced under $\rm H_2$ to a mixture of cyclopentanes with high octane ratings, density and flow properties required for a synthetic fuel [14]. LA dimerization using an acidic cation-exchange resin catalyst and then hydrogenation with Pd is reported in patent literature [15]. In another example Paniagua and coworkers have used a propyl sulfonic acid modified SBA-15 as a catalysts for LA dimerization [8]. More recently the same research group have discovered a cooperative effect between strong Brønsted and Lewis acid sites of zeolites in promoting LA dimerization [6]. Furthermore, comparable Brønsted - Lewis acid cooperative effects in LA dimerization is known in a homogeneous system $\rm CCl_3CO_2H$ - $\rm ZnCl_2$ as well [10]. In a more recent example, Chen et al. reported a $\rm H_2/Pd/C$ - $\rm H_3PO_4$ reduction of LA-furfural condensation product as an approach for producing long chain hydrocarbons [16].

Our efforts on catalytic upgrading of renewable feedstocks have also contributed in opening new pathways for upgrading LA to a number of C7-C10 feedstocks [17–21]. For example, an acid catalyzed aldol condensation between LA and glyoxylic acid could be used to prepare a C7 polymer building block 1-methyl-2,8-dioxabicyclo[3.3.0]oct-4-ene-3,7-dione [17]. In another study, we reported the synthesis of 2,9,11,14-tetraoxadispiro[4.1.5.3]pentadecane-3,6-dione in excellent yields by Amberlyst-H $^+$ and $\rm H_2SO_4$ catalyzed condensations of LA with paraformaldehyde [22]. In addition, we have explored the base catalyzed condensation between LA and 5-hydroxymethylfurfural and observed the formation of (*E*)-6-[5-(hydroxymethyl)furan-2-yl]-hex-4-

^{*} Corresponding author at: Department of Chemistry, Prairie View A&M University, 700 University Drive, Prairie View, TX 77446, USA. E-mail address: asamarasekara@pvamu.edu (A.S. Amarasekara).

oxo-5-enoic acid and (*E*)-3-[5-(hydroxymethyl)furan-2-yl]methylene-4-oxo-pentanoic acid in 82% total yield. [23]. Recently, we have studied the acid catalyzed self condensation of LA using solid acids, where tetrahydro-2-methyl-5, γ -dioxo-2-furanpentanoic acid was identified as the major product and diastereomeric pairs of 3-(2-methyl-5-oxo-tetrahydrofuran-2-yl)-4-oxopentanoic acid and 3-acetyl-2-methyl-tetrahydro-5-oxo-2-furanpropanoic acid were the minor products [18]. SiO₂-SO₃H was the most effective catalyst among acids studied giving a 56% total yield [18].

The use metal chelates or oxide-based catalysts in aldol dimerization is rare and most upgrading methods require two steps for condensation and reduction. Interestingly we have noted that most challenging task is the deoxygenation and combining this step into the condensation. Following up on our previous work and inspired by the Grilic and coworkers recent results in using NiMo/Al₂O₃ catalyst under H₂ to achieve a one-pot dimerization and decarboxylation of LA [13], we have studied the use of $LiNi_xMn_yCo_zO_2$ on carbon catalyst derived from spent Li-ion batteries. This no-cost or inexpensive mixed metal oxide catalyst was prepared by pyrolyzing electrode coatings of a spent Li-ion DELL 1525 laptop battery at 600 °C in air. Furthermore, we have recently shown the application of this waste material as an efficient reusable catalyst for oxidation of cellulose derived biofurans to their value-added oxidation products [24]. In addition, the same catalyst could be used for oxidation of D-glucose to a mixture of glycolic, tartaric, malic, 2-hydroxybutaric and succinic acids [25]. In continuation of our efforts in development of LA upgrading methods for producing sustainable fuel and polymer feedstocks we have studied the use of LiNixMnvCozO2 on carbon as a new catalyst for one-pot reductive - dimerization of LA. Furthermore, transition metals Ni, Mn and Co are well known for their catalytic activities and can be cost-efficient alternatives to noble metals [21,26]. In this publication we describe the formation of a series of C9 and C6 products in a new single-reactor decarboxylative - dimerization process of LA by the use of no-cost catalyst as well as the commercially available fresh LiNixMnyCo_zO₂.

The market price of pure lithium nickel manganese cobalt oxide can vary depending on the metal ratio and the average is about \$ 2 per gram. In comparison, spent battery waste based catalyst LiBBM-600 described in this publication is a nearly no-cost material with only labor cost for separation of electrode coatings from used batteries and energy cost associated with pyrolysis of LiBBM. Similar to our work Liang et al. have recently reported a valuable application of Li-ion battery waste material. In this instance, electrode coatings from used Li-ion batteries were used in preparation of $CoFe_2O_4$ [27], and $MnFe_2O_4$ [28]. More importantly, these magnetically separable ferrite materials could be used for efficient degradation of toxic bisphenol A; furthermore, the used battery waste derived ferrites were reported as more cost-effective than the original materials [27,28].

2. Experimental

2.1. Materials and instrumentation

Levulinic acid (> 99%) and dichloromethane were purchased from Aldrich Chemical Co. Li_{1.0}Ni_{0.3}Co_{0.3}Mn_{0.3}O₂ (NCM-111) was purchased from HuNan Changyuan LiCo. Ltd., China. LiBBM-600 catalyst was prepared by pyrolysis of pooled cathode and anode electrode coating black material collected from a spent DELL 1525 laptop battery (87 Wh, 11.1 V) as shown in Fig. 1 and described in our previous work [25]. The catalyst was pyrolyzed in a Thermo Scientific Lindberg Blue M Mini-Mite tube furnace by placing the sample in a quartz tube. LiBBM-600 was analyzed using ATR-IR, SEM, EDX and powder X-ray crystallography analysis of LiBBM-600 confirmed the composition with Ni, Co and Mn, indicating the presence of lithium nickel manganese cobalt oxide (LiNi_xCo_yMn_zO₂) loaded on graphite carbon. Scanning Electron Microscopy (SEM) was carried out using a FEI Quanta 400 ESEM instrument and imaging was performed with a secondary electron detector operating at a 20 kV accelerating voltage. Parr Instrument Co. reactor with a 50 mL 4720 stainless-steel pressure vessel, 4838 reactor temperature controller, was used to perform all high pressure reactions. These experiments were carried out without stirring. The reaction products were analyzed using a Bruker 436-GC/EVOQ GC-MS with an auto-sampler. Reaction products were dissolved in dichloromethane (~ 20 mg/mL) filtered through a $0.22 \, \mu m$ filter and $1 \, \mu L$ samples were injected using an auto-injector for the analysis.

2.2. General procedure for the LiBBM-600 and NCM-111 catalyzed decarboxylative - dimerization of levulinic acid

Levulinic acid (116 mg, 1.0 mmol) was mixed with solid acid catalyst (4–10 w/w %) in the 50 mL Parr reactor, closed, flushed with hydrogen three times and pressurized to 1.24 MPa (180 psi). Then the reactor was quickly heated and maintained at the desired temperature using 4838 temperature controller. After the reaction period reactor was cooled to room temperature diluted with dichloromethane and filtered using a fine glass sinter. The filtrate was further diluted to 10.00 mL and analyzed by injecting 1 μ L to Bruker 436-GC/EVOQ GC–MS using an auto-sampler. The unreacted levulinic acid content in the reactions was determined by standard addition method. The catalyst loading, reaction conditions, initial H₂ pressure, LA conversion and Total Ion Current (TIC) area ratio of products with MW 100: 152: 154 are shown in Table 1. LA conversion was calculated using the formula:

 $LA\,Conversion\,(\%) = \frac{\text{mol of levulinic used} - \text{mol of levulinic unreacted}}{\text{mol of levulinic used}}\,x\,100\%$



- Mechanical separation of cathode and anode coatings
- 2. 600 °C, 30 min., air

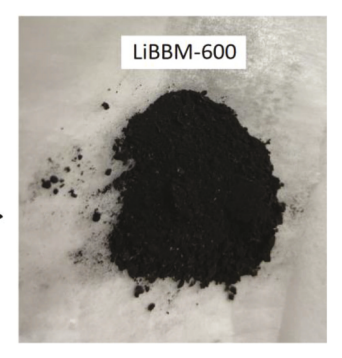


Fig. 1. Preparation of Lithium ion Battery Black Material - 600 (LiBBM-600) catalyst from 18,650 Li-ion battery cells in a discharged spent DELL 1525 laptop battery (87 Wh, 11.1 V).

Table 1
Catalyst (loading w/w %), reaction conditions, H₂ pressure, LA conversion (%) and C6, C9 product (%) in LiBBM-600 and NCM-111 catalyzed decarboxylative - dimerization of levulinic acid under hydrogen atmosphere. All reactions were carried out without a solvent.

Entry	Catalyst (loading w/w %)	Reaction conditions temperature, time	H ₂ Pressure (MPa)	LA conversion (%)	TIC area ratio of products with MW 100: 152: 154
1	LiBBM-600 (10)	100 °C, 15 h	1.00	18	-: 48: 52
2	LiBBM-600 (10)	120 °C, 15 h	1.24	62	-: 46: 54
3	LiBBM-600 (10)	150 °C, 15 h	1.24	71	30: 32: 38
4	LiBBM-600 (8)	140 °C, 15 h	1.24	93	26: 34: 40
5	LiBBM-600 (10)	140 °C, 15 h	1.24	94	27: 35: 38
6	NCM-111 (4)	130 °C, 30 h	1.24	50	-: 49: 51
7	NCM-111 (6)	130 °C, 30 h	1.24	77	-: 42: 58
8	NCM-111 (8)	130 °C, 30 h	1.24	84	-: 43: 57
9	NCM-111 (4)	140 °C, 30 h	1.24	85	-: 44: 56

2.3. Recyclability of the LiBBM-600 catalyst in the decarboxylative - dimerization of levulinic acid

Levulinic acid (2.000 g, 17.2 mmol) was mixed with solid acid catalyst (200 mg, 10% w/w) in the 50 mL Parr reactor, closed, flushed with hydrogen for three times and pressurized to 1.24 MPa (180 psi) and heated at 140 °C for 15 h. After the reaction period reactor was cooled to room temperature diluted with 5.00 mL of methanol and centrifuged at 1700g for 15 min. to remove the catalyst. The catalyst was washed with 10.00 mL of methanol and combined supernatant was analyzed using GC–MS as in the previous experiment. The catalyst recovered was first dried in an oven at 100 °C for 24 h and then pyrolyzed at 600 °C in air for 30 min. Using Thermo Scientific Lindberg Blue M Mini-Mite tube furnace. The recycled catalyst was allowed to cool to room temperature and used for the dimerization of levulinic acid following the same procedure. The LA conversions for four catalytic cycles are shown in Table 2.

3. Results and discussion

3.1. LiBBM-600 catalyst preparation and characterization

A spent DELL 1525 laptop battery was completely discharged by immersing in 10% (w/w) aqueous sodium chloride solution for six days. Nine 18,650 cells in the battery were removed and cathode and anode black electrode coatings were mechanically separated and combined, dried in air for 5 days to give 46 g lithium ion battery black material (LiBBM). This black powder was pyrolyzed in air at 600 $^{\circ}$ C, for 30 min. Using a Thermo Scientific Lindberg Blue M Mini-Mite tube furnace and by placing the sample in a quartz tube. Then the sample was cooled to room temperature, grounded and sieved through a number 25 mesh (710 µm) to give 38 g fine black powder catalyst named as LiBBM-600. This product was characterized using ATR-IR, SEM, EDX and powder Xray. The ATR-IR, powder X-ray spectrographs are shown in our previous publication [25]; additionally, SEM and EDX elemental analysis of this sample as well as SEM and EDX of commercially available NCM111 are shown in Fig. 2 for comparison. In our previous work we have compared the LiBBM and the pyrolysis product LiBBM-600 using attenuated total reflection infrared (ATR-IR) spectroscopy [25]. These before and after spectra showed no changes to the major component graphite carbon due to the pyrolysis at 600 °C [25].

The SEM image of LiBBM-600 shown in Fig. 2a indicates a non-

Table 2Levulinic acid conversion and C6, C9 product Total Ion Current (TIC) area ratio in LiBBM-600 catalyst recycling.

Cycle	LA conversion (%)	TIC area ratio of products with MW 100: 152: 154
1	94	27: 35: 38
2	32	28: 36: 36
3	19	26: 36: 38

homogeneous surface with 1-2 µm shiny metal or metal oxide clusters on a dull carbon support. The Energy Dispersive X-ray Spectroscopy (EDX) analyses of this LiBBM-600 catalyst sample show peaks: C, O, Al, P, Mn, Co and Ni as shown in the plot in Fig. 2b and in the elemental mass and atom compositions are tabulated below. Nevertheless, lithium expected in LiBBM-600 was not observed, because EDX is not sensitive to lithium. The other expected elements Mn, Co, Ni is present most likely as oxides as well the carbon in the graphite form used as the conductor in electrode coating. The Al in sample may be due to a contamination from aluminum foil used in cathode and P is possibly from residual electrolyte in the cells. The elemental composition in LiBBM-600 sample is most probably due to the presence of lithium nickel manganese cobalt oxide (LiNi_xCo_yMn_zO₂) as the active material in the laptop battery cells. Moreover, the empirical composition of the transition elements with anticipated catalytic activity is in the ratio: Ni: Co: Mn 2.02: 0.73: 1.00 as point out in the EDS data in Fig. 2b. In an attempt to compare the catalytic activity of spent Li-ion battery derived LiBBM-600 with pristine lithium nickel cobalt manganese oxide sample we have selected commercially available NCM-111. The SEM and EDX analyses of NCM-111 are shown in Fig. 2c and d respectively. The SEM image of NCM-111 shows a mixture of ${\sim}10~\mu m$ spheres with rough surfaces and 2–5 μm irregular shaped lumps in picture 2c. The transition element ratio of the NCM-111 sample can be calculated from the EDX data in Fig. 2d and composition table below. It is important to note that the NCM-111 sample selected for catalytic activity comparison showed a transition element ratio of Ni: Co: Mn 1.58: 0.61: 1.00, which is somewhat comparable to LiBBM-600.

3.2. LiBBM-600 and NCM-111 catalyzed decarboxylative - dimerization of levulinic acid under hydrogen atmosphere

Levulinic acid dimerization reaction under hydrogen atmosphere was first tested using spent Li-ion battery derived LiBBM-600 catalyst. Then the catalytic activity of this no or low-cost catalyst was compared with a commercially available pristine lithium nickel cobalt manganese oxide of comparable transition metal composition. The catalyst used loading, reaction conditions, initial H₂ pressure, LA conversion and Total Ion Current (TIC) peak area ratios of products with MW 100: 152: 154 are shown in Table 1.

Initial experiments with 10% (w/w) LiBBM-600 catalyst loading and at temperatures in the 100–120 °C range for 15 h yielded low LA conversions of 18 and 62% as shown in entries 1 and 2 in Table 1. Increasing the temperature to 150 °C, keeping the catalyst loading at 10% improved the LA conversion to 71%. These experiments resulted a mixture of five significant products in leaving significant amount of unreacted levulinic acid. The mass spectra of the five products showed molecular ions at m/e of either 152 or 154. While changing reaction conditions to improve the LA conversion, we have lowered the temperature to 140 °C, keeping the heating time at 15 h and catalyst loading to 8% (w/w) LiBBM-600. This experiment resulted an excellent 93% conversion to levulinic acid as shown in entry 4; however, the product

(a). LiBBM-600

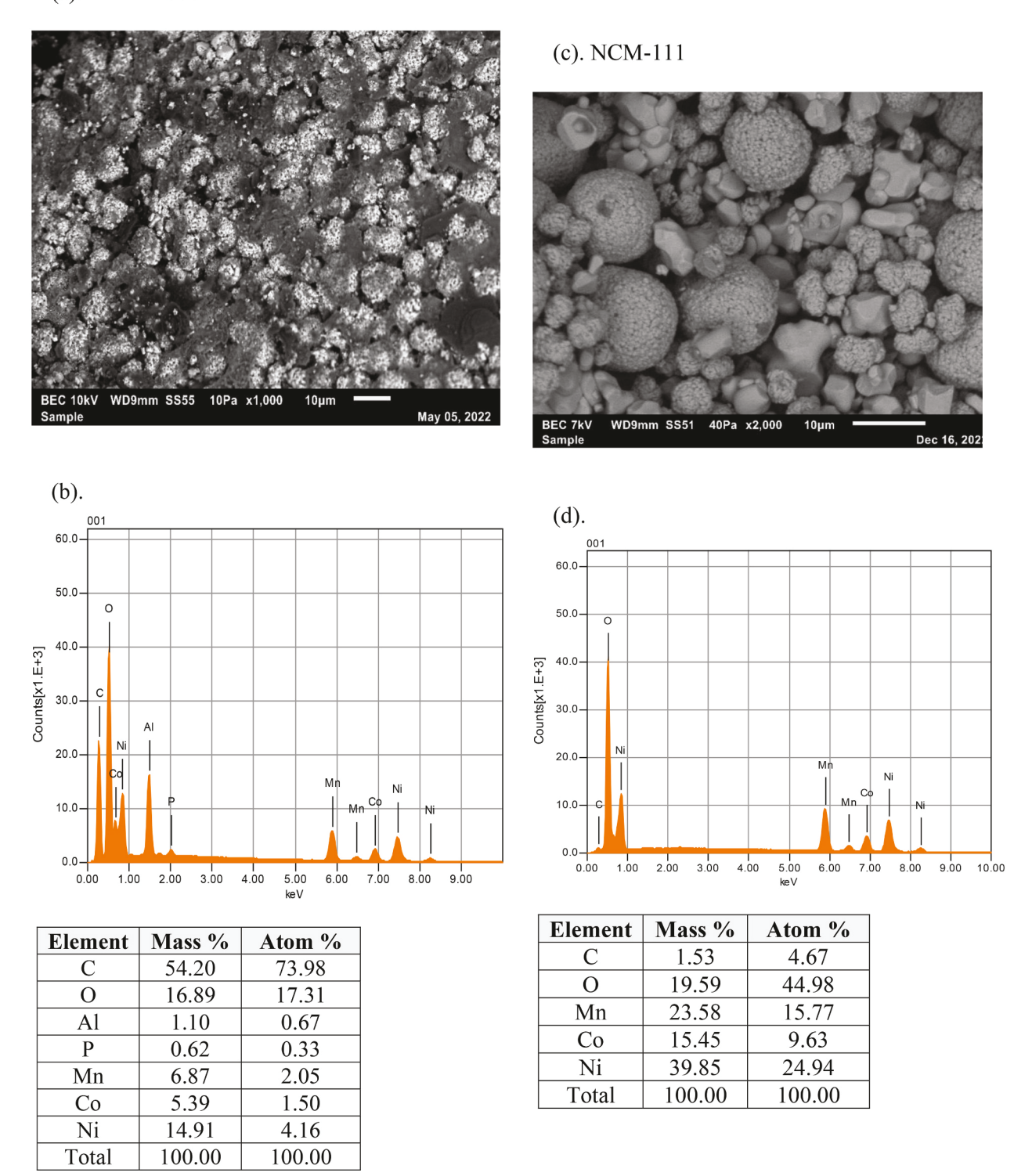


Fig. 2. (a). Scanning electron microscopy (SEM) of LiBBM-600 (b). Energy Dispersive X-ray Spectroscopy (EDX) analyses of LiBBM-600 (c). Scanning electron microscopy (SEM) of NCM111 (d). Energy Dispersive X-ray Spectroscopy (EDX) analyses of NCM111.

composition changed, as a new product peak of shorter retention time of 3.650 min. With m/e of 100 was also observed in addition to the five products of m/e of either 152 or 154. In further optimization of the yield LiBBM-600 catalyst loading was increased to 10% keeping the reaction temperature and time at 140 $^{\circ}$ C, 15 h, as in the previous experiment. This experiment produced the highest LA conversion of 94% as shown under entry 5. The GC–MS total ion current profile of this experiment is

shown in Fig. 3, and the mass spectra of the six products and unreacted starting material levulinic acid are shown in supplementary material.

In an attempt to validate the lithium nickel cobalt manganese oxide as the active catalyst in LiBBM-600 we have experimented with a commercially available pristine lithium nickel cobalt manganese oxide of the type NCM-111. The results from experiments using NCM-111 as catalyst are shown as entries 6–9 in Table 1. In early experiments,

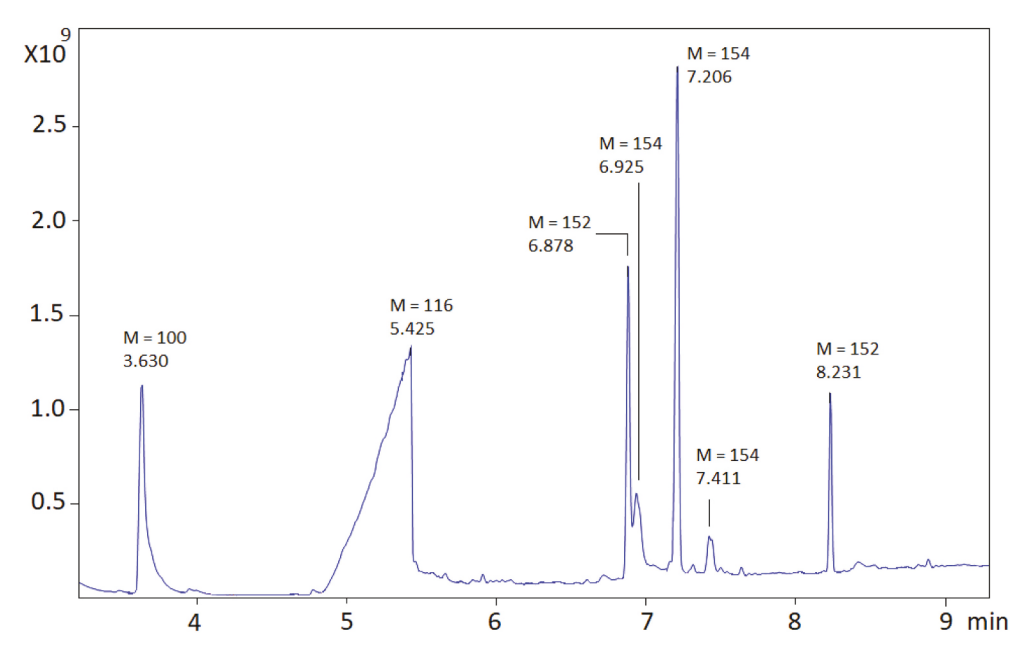


Fig. 3. Representative total ion current chromatogram of the product from GC–MS experiment in entry 5, Table 1. 10% w/w LiBBM-600 catalyst loading, 1.24 MPa H₂, 140 °C, 15 h. Retention times and molecular ions for significant peaks are shown. The mass spectra of the GC–MS peaks are in the supplementary material.

relatively smaller catalyst loadings and lower temperatures were attempted with NCM-111 as this is a pure mixed metal oxide without a catalyst support. The NCM-111 experiment with 4, 6 and 8% catalyst loading and 130 $^{\circ}$ C, 30 h reactions resulted 50, 77 and 84% conversions. In continuation of optimization, 85% LA conversions could be achieved with the use 4% catalyst loading and increasing the temperature to 140 $^{\circ}$ C and allowing for 30 h reaction. Interestingly none of the NCM-111 catalyzed experiments resulted the retention time 3.630 min. Low molecular weight m/e 100 product and only m/e 152 and 154 products were observed with this neat mixed metal oxide catalyst.

Representative total ion current (TIC) chromatogram of the product from GC–MS experiment in entry 5, Table 1 is shown in Fig. 3. The GC–MS profile shows levulinic acid as a broad peak at 5.425 min. This peak was confirmed by co-injection. In addition, injecting the product in methylene chloride after washing with a dilute aqueous NaOH solution eliminated this peak, further confirming as an acidic compound. Six product peaks were observed, including: 3.630 min. MW = 100; 6.878, 8.231 min. MW = 152 peaks and 6.925, 7.206, 7.411 min. MW = 154 peaks. The mass spectra of these GC–MS peaks are in the supplementary material.

Proposed reaction pathways to explain the formation of C9 products and a C6 product as in Table 1 are shown in Fig. 4. Levulinic acid can be enolized to give C5 or C3 enolates. These enolates next undergoes aldol condensations with another molecule of levulinic acid to give aldol dimer products 2 and 3 respectively. In the next step these dicarboxylic acids may undergo decarboxylation with the loss of carbondioxide. The decarboxylation of one acid group in intermediate 2 leaving the other intact can give monocarboxylic acids 4 and 7. These hydroxy-keto-acids can lactonize in two different modes producing di-hydroxy-lactone 5 and keto-lactone 8. A double dehydration of 5 can give 6, $C_9H_{12}O_2$ with MW 152. On the other path, hydrogenation followed by dehydration can lead to 9, $C_9H_{14}O_2$ with MW 154.

In the middle section of the scheme, alternative decarboxylation paths of **3** can produce intermediates **10** and **13**. These two intermediates can also lactonize to **11** and **14**. The double dehydration of **11** will lead to **12**, $C_9H_{12}O_2$ with MW 152; whereas reduction and dehydration of **14** can result **15**, $C_9H_{14}O_2$ with MW 154. The four C9 unsaturated lactone products: **6**, **9**, **12** and **15** shown in proposed scheme may isomerize to a number of isomers and it is not possible to assign the precise isomer from the total ion current GC–MS peaks or

from the mass spectroscopy data available in this analysis. The three MW 154 peaks in the GC–MS profile in Fig. 3 is likely due to a cis/trans isomerization of one of the $C_9H_{12}O_2$ product shown in reaction mechanism.

The double decarboxylation with the loss of two carbon dioxide molecules from aldol adduct 3 may lead to the C8 product 16 shown in the far right scheme in Fig. 4. The fragmentation of 16 with the loss of ethane may give 1,3-diketone 17. A series of follow up reactions of 17 with reduction, dehydration to give intermediate 18 is followed by a second reduction leads to 19 with formula $C_6H_{12}O$ and MW 100. This unsaturated alcohol was observed only in experiments shown as entries 4 and 5 in Table 1. The mass spectrum of 19 showed the M-1 molecular ion peak at m/e 99 as expected for an alcohol. The mass spectra of all C9 unsaturated lactones and the C6 unsaturated alcohol are included in the supplementary material.

Aldol condensation of LA and decarboxylation of the product in a single reactor process is reported only with NiMo/Al₂O₃ catalyst under H₂ [13]. However, decarboxylation of fatty acids to long chain alkanes as well as fragmentation of products are known with a variety of catalysts. Nevertheless, in most cases expensive Pt, Pd, or Rh noble metal catalysts with hydrogen, high temperature and pressure conditions were used in these decarboxylation experiments as shown in examples in Table 4. Furthermore, decarboxylation of LA to n-butane is also known with the use of Pt on carbon as catalyst (entry 5, Table 4). Therefore, in comparison to examples shown in Table 4, the new LiBBM-600 catalyst has certain cost-advantage as well as the rare ability to promote aldol condensation and deoxygenation in a single reactor process.

3.3. Reuse of LiBBM-600 catalyst in decarboxylative - dimerization of levulinic acid

The levulinic acid conversion and C6, C9 product TIC composition in LiBBM-600 catalyst recycling are shown in Table 2. This experiment clearly indicates that catalyst activity is significantly lost in attempts to reuse the LiBBM-600 catalyst. The levulinic acid conversion dropped from 96% to 32% in first reuse and further to 19% in the second reuse suggesting poor recyclability of the catalyst. However, the C6, C9 product ratio remains practically the same, suggesting that catalyst composition remains the same in reuse of the catalyst.

Energy Dispersive X-ray Spectroscopy (EDX) analyses of LiBBM-600

Fig. 4. Proposed reaction pathways for the formation of C9 lactone products and C6 unsaturated alcohol product by LiBBM-600 and NCM-111 catalyzed decarboxylative - dimerization of levulinic acid under hydrogen atmosphere.

Table 3Energy Dispersive X-ray Spectroscopy (EDX) analyses of LiBBM-600 catalyst recovered after 1st cycle of use.

Element	Mass %	Atom %
С	55.87	74.84
0	17.85	17.68
Al	1.02	0.61
P	0.51	0.25
Mn	6.12	1.77
Co	4.89	1.33
Ni	13.74	3.52
Total	100	100

catalyst recovered after 1st cycle and pyrolysis at 600 $^{\circ}$ C in air for 30 min. is shown in Table 3. In comparison to the elemental composition of fresh LiBBM-600 catalyst shown in fig. 2b, the recycled catalyst shows a small increase in mass and atom percentages of carbon and oxygen. In contrary mass percentages of Mn, Co and Ni are slightly decreased. However, the relative ratios of these metals remain practically the same after recycling.

4. Conclusion

We have revealed that pyrolyzed electrode coating material from battery cells in a spent DELL 1525 laptop Li-ion battery can be used as a catalyst for decarboxylative - dimerization of levulinic acid to a mixture of C9 and C6 products in over 90% conversion of levulinic acid. In

Table 4Selected literature examples of catalytic decarboxylations of aliphatic carboxylic acids.

Entry	Decarboxylation reaction	Catalyst and conditions	Reference
1	Srearic, oleic and palmitic acids to hydrocarbons, 60-85% conversion	Pd-ZSM-5 zeolite, 250C, H2 6 bar	[29]
2	Palmitic acid to pentadecane 55% yield	5% Pt—C, 290°C, 1.5h.	[30]
3	Fatty acids to C7-C17 alkanes	5% Ru—C, H2	[31]
4	Fatty acid to alkanes	Rh - Si nanowire array, H2 10 bar, 200C, MW ~ 40 W	[32]
5	Levulinic acid to n-butane, 95.5% yield	Pt-C, 300C, 4 h	[33]
6	Stearic acid to heptadecane, 47% yield	Ni-Mordenite zeolite	[34]

preparation of the catalyst, mechanically separated electrode coating from used Li-ion battery cells was pyrolyzed at 600 °C to remove electrolytes and binders and this single step heat treatment provides a simple method to prepare an inexpensive ready-made catalyst with Li, Ni, Co and Mn mixed oxide on carbon. In addition we have proven that lithium nickel manganese cobalt oxide (LiNi_xCo_yMn_zO₂) as the active ingredient in the waste battery material derived catalyst by showing that pristine commercially available LiNi_xCo_yMn_zO₂ is equally effective in catalyzing the transformation. However, attempts to reuse the catalyst after regeneration by pyrolysis at 600 °C resulted poor yields even after first cycle. We are currently exploring the ways for improving the recyclability of these catalysts. In conclusion we have developed an inexpensive non-noble metal based catalyst system for efficient dimerization of levulinic acid to C9 compounds through unpresecedented concurrent decarboxylation, with potential applications in producing sustainable fuels or fuel precursors.

Declaration of Competing Interest

The authors declare that they have no known competing financial interests or personal relationships that could have appeared to influence the work reported in this paper.

Data availability

No data was used for the research described in the article.

Acknowledgements

We thank United States National Science Foundation (NSF) grants CBET-1704144, HRD-1036593, USDA-NIFA grant 12684238: Award No. 2020-65209-31474 and Welch Foundation grant L0002 - 20181021 for financial support. The GC-MS instrument used was acquired through DOD HBCU-MSI grant W911NF2110167.

Appendix A. Supplementary data

Supplementary data to this article can be found online at https://doi.org/10.1016/j.fuproc.2023.107913.

References

- [1] W.P. Xu, X.F. Chen, H.J. Guo, H.L. Li, H.R. Zhang, L. Xiong, X.D. Chen, Conversion of levulinic acid to valuable chemicals: a review, J. Chem. Technol. Biotechnol. 96 (2021) 3009–3024.
- [2] F. Deng, A.S. Amarasekara, Catalytic upgrading of biomass derived furans, Ind. Crop. Prod. 159 (2021), 113055.
- [3] L.D. Mthembu, R. Gupta, N. Deenadayalu, Advances in Biomass-based Levulinic Acid Production, Waste Biomass Valoriz. 14 (2023) 1–22.
- [4] R. Ukawa-Sato, N. Hirano, C. Fushimi, Design and techno-economic analysis of levulinic acid production process from biomass by using co-product formic acid as a catalyst with minimal waste generation, Chem. Eng. Res. Design 192 (2023) 389-401.
- [5] A. Yousuf, M.A. Rahman, M.J. Rahman, M.S. Hossain, Chapter 6 Role of catalysts in sustainable production of biojet fuel from renewable feedstocks, in: A. Yousuf, C. Gonzalez-Fernandez (Eds.), Sustainable Alternatives for Aviation Fuels, Elsevier, 2022, pp. 125–176.
- [6] P. Juárez, C. López-Aguado, M. Paniagua, J.A. Melero, R. Mariscal, G. Morales, Self-condensation of levulinic acid into bio-jet fuel precursors over acid zeolites:

- Elucidating the role of nature, strength and density of acid sites, Appl. Catal. A Gen. 631 (2022), 118480.
- [7] Q. Zhang, J. Xiao, J. Hao, Q. Wu, G. Song, Energy and exergy analyses of bio-jet fuel production from full components in lignocellulosic biomass via aqueous-phase conversion, Appl. Therm. Eng. 201 (2022), 117723.
- [8] M. Paniagua, F. Cuevas, G. Morales, J.A. Melero, Sulfonic mesostructured SBA-15 silicas for the solvent-free production of bio-jet fuel precursors via aldol dimerization of levulinic acid, ACS Sustain. Chem. Eng. 9 (2021) 5952–5962.
- [9] F. Laura, D. Eva, O. Salvador, Base-catalyzed condensation of levulinic acid: a new biorefinery upgrading approach, ChemCatChem 8 (2016) 1490–1494.
- [10] Z. Li, J. Zhang, M.M. Nielsen, H. Wang, C. Chen, J. Xu, Y. Wang, T. Deng, X. Hou, Efficient C–C bond formation between two levulinic acid molecules to produce C10 compounds with the cooperation effect of Lewis and Brønsted Acids, ACS Sustain. Chem. Eng. 6 (2018) 5708–5711.
- [11] E. Mäkelä, J.L. Gonzalez Escobedo, M. Lindblad, M. Käldström, H. Meriö-Talvio, H. Jiang, R.L. Puurunen, R. Karinen, Hydrodeoxygenation of levulinic acid dimers on a zirconia-supported ruthenium catalyst, Catalysts 10 (2020) 200.
- [12] L. Faba, E. Díaz, S. Ordóñez, Base-catalyzed condensation of levulinic acid: a new biorefinery upgrading approach, ChemCatChem 8 (2016) 1490–1494.
- [13] M. Grilc, B. Likozar, Levulinic acid hydrodeoxygenation, decarboxylation and oligmerization over NiMo/Al2O3 catalyst to bio-based value-added chemicals: Modelling of mass transfer, thermodynamics and micro-kinetics, Chem. Eng. J. 330 (2017) 383–397.
- [14] Z. Li, A.L. Otsuki, M. Mascal, Production of cellulosic gasoline via levulinic ester self-condensation, Green Chem. 20 (2018) 3804–3808.
- [15] R. Blessing, L. Petrus, Process for the dimerisation of levulinic acid, dimers obtainable by such process and esters of such dimers, US Patent US20060135793A1, 2006.
- [16] L. Chen, Y. Liu, X. Zhang, J. Liu, Q. Zhang, L. Ma, Catalytic production of longchain hydrocarbons suitable for aviation turbine fuel from biomass-derived levulinic acid and furfural, Fuel 334 (2023), 126665.
- [17] A.S. Amarasekara, U. Ha, Acid catalyzed condensation of levulinic acid with glyoxylic acid: synthesis of 1-methyl-2,8-dioxabicyclo[3.3.0]oct-4-ene-3,7-dione, Tetrahedron Lett. 57 (2016) 2598–2600.
- [18] A.S. Amarasekara, B. Wiredu, T.L. Grady, R.G. Obregon, D. Margetic, Solid acid catalyzed aldol dimerization of levulinic acid for the preparation of C10 renewable fuel and chemical feedstocks, Catal. Commun. 124 (2019) 6–11.
- [19] A.S. Amarasekara, S.A. Hawkins, Synthesis of levulinic acid-glycerol ketal-ester oligomers and structural characterization using NMR spectroscopy, Eur. Polym. J. 47 (2011) 2451–2457.
- [20] A.S. Amarasekara, B. Wiredu, Acidic ionic liquid catalyzed one-pot conversion of cellulose to ethyl levulinate and levulinic acid in ethanol-water solvent system, BioEnergy Res. 7 (2014) 1237–1243.
- [21] A.S. Amarasekara, Y.M. Lawrence, Raney-Ni catalyzed conversion of levulinic acid to 5-methyl-2-pyrrolidone using ammonium formate as the H and N source, Tetrahedron Lett. 59 (2018) 1832–1835.
- [22] A.S. Amarasekara, U. Ha, M.S. Fonari, S.N. Bejagam, D. Margetic, Sulfuric acid and Amberlyst-H+ catalyzed condensation reactions of renewable keto acids with paraformaldehyde: synthesis of a new dispiro bis-lactone ring system 2,9,13trioxadispiro[4.1.4.3]tetradecane-3,6,10-trione, RSC Adv. 7 (2017) 23917–23923.
- [23] A.S. Amarasekara, T.B. Singh, E. Larkin, M.A. Hasan, H.-J. Fan, NaOH catalyzed condensation reactions between levulinic acid and biomass derived furanaldehydes in water, Ind. Crop. Prod. 65 (2015) 546–549.
- [24] A.S. Amarasekara, S.K. Pinzon, T. Rockward, H.N.K. Herath, Spent Li-ion battery electrode material with lithium nickel manganese cobalt oxide as a reusable catalyst for oxidation of biofurans, ACS Sustain. Chem. Eng. 10 (2022) 12642–12650.
- [25] A.S. Amarasekara, H.N.K. Herath, T.L. Grady, C.D. Gutierrez Reyes, Oxidation of glucose to glycolic acid using oxygen and pyrolyzed spent Li-ion battery electrode material as catalyst, Appl. Catal. A Gen. 648 (2022), 118920.
- [26] A.S. Amarasekara, I. McNeal, J. Murillo, D. Green, A. Jennings, A simple one-pot synthesis of Jacobson-Katsuki type chiral Mn(III)-salen catalyst immobilized in silica by sol-gel process and applications in asymmetric epoxidation of alkenes, Catal. Commun. 9 (2008) 2437–2440.
- [27] J. Liang, Y. Xue, J.-N. Gu, J. Li, F. Shi, X. Guo, M. Guo, X. Min, K. Li, T. Sun, J. Jia, Sustainably recycling spent lithium-ion batteries to prepare magnetically separable cobalt ferrite for catalytic degradation of bisphenol a via peroxymonosulfate activation, J. Hazard. Mater. 427 (2022), 127910.
- [28] J. Liang, M. Guo, Y. Xue, J.-N. Gu, J. Li, F. Shi, X. Guo, X. Min, J. Jia, K. Li, T. Sun, Constructing magnetically separable manganese-based spinel ferrite from spent ternary lithium-ion batteries for efficient degradation of bisphenol a via peroxymonosulfate activation, Chem. Eng. J. 435 (2022), 135000.

- [29] M. Arroyo, L. Briones, H. Hernando, J.M. Escola, D.P. Serrano, Selective decarboxylation of fatty acids catalyzed by Pd-supported hierarchical ZSM-5 zeolite, Energy Fuel 35 (2021) 17167–17181.
- [30] I. Edeh, T. Overton, S. Bowra, Renewable diesel production by hydrothermal decarboxylation of fatty acids over platinum on carbon catalyst, Biofuels 12 (2021) 945–952.
- [31] J. Zhang, X. Huo, Y. Li, T.J. Strathmann, Catalytic hydrothermal decarboxylation and cracking of fatty acids and lipids over Ru/C, ACS Sustain. Chem. Eng. 7 (2019) 14400–14410.
- [32] H. Baek, K. Kashimura, T. Fujii, S. Tsubaki, Y. Wada, S. Fujikawa, T. Sato, Y. Uozumi, Y.M. Yamada, Production of bio hydrofined diesel, jet fuel, and carbon
- monoxide from fatty acids using a silicon nanowire array-supported rhodium nanoparticle catalyst under microwave conditions, ACS Catal. $10\ (2020)\ 2148-2156$.
- [33] J. Jiang, T. Li, K. Huang, G. Sun, J. Zheng, J. Chen, W. Yang, Efficient preparation of bio-based n-butane directly from levulinic acid over Pt/C, Ind. Eng. Chem. Res. 59 (2020) 5736–5744.
- [34] J.M. Crawford, S.F. Zaccarine, N.C. Kovach, C.S. Smoljan, J. Lucero, B.G. Trewyn, S. Pylypenko, M.A. Carreon, Decarboxylation of stearic acid over Ni/MOR catalysts, J. Chem. Technol. Biotechnol. 95 (2020) 102–110.